Electronic Supplementary Information

Bioconversion of wastewater-derived cresols to methyl muconic acids for use in performance-advantaged bioproducts

William R. Henson,[a,‡] Nicholas A. Rorer,[a,‡] Alex W. Meyers,[a,‡] Caroline B. Hoyt,[a] Heather B. Mayes,[a] Jared J. Anderson,[a] Brenna A. Black,[a] Lahiru Jayakody,[a] Rui Katahira,[a] William E. Michener,[a] Todd VanderWall,[a] Davinia Salvachúa,[a] Christopher W. Johnson,[a] and Gregg T. Beckham[a,*]

a. Renewable Resources and Enabling Sciences Center, National Renewable Energy Laboratory, Golden CO 80401;
* Corresponding author. Email: gregg.beckham@nrel.gov
‡ Denotes equal contribution

Materials and methods

Materials

Unless otherwise noted, reagents were purchased from Sigma-Aldrich and used as is.

Strains and plasmids

All strains and plasmids used in this work are listed in Table S1. For plasmid construction, Q5® Hot Start High-Fidelity 2X Master Mix and Gibson Assembly® Master Mix from New England Biolabs (NEB) and primers produced by Integrated DNA Technologies were used. Primers and synthesized DNA sequences are listed in Tables S2-S3. Genomic integrations were performed using pK18sB[1] using sacB counterselection with ~800-1000 bp homology arms on each side of the integration site.[2] New ribosome binding site (RBS) sequences were designed using the RBS calculator,[3] and codon optimization of heterologous genes was performed using OPTIMIZER.[4] Plasmids were transformed into *E. coli* 5-alpha F' I^q cells (NEB) and selected on Luria Broth (LB) agar plates supplemented with 50 μg/mL kanamycin and grown at 37°C. Sanger sequencing was used to confirm all assembled constructs. *P. putida* KT2440 (ATCC 47054) was used as the basis of strain engineering. Electrocompetent *P. putida* KT2440 cells were prepared following a modified protocol from Choi *et al*.[5] Electrocompetent transformations and genomic integrations were performed as previously described.[2]

Chemical characterization by NMR spectroscopy

Nuclear magnetic resonance (NMR) spectra were recorded on a Bruker AVANCE 400 MHz spectrometer equipped with a 5 mm BBO probe. A pulse sequence encompassing water suppression was utilized. For quantification of 2-methyl muconic acid, culture supernatants were diluted ten-fold in deuterium oxide (D_2O) and 0.1 mM trimethylsilylpropanoic acid (TMSP) was used as an external proton standard. Deuterated DMSO or chloroform was used for the quantification of the acids and esters of muconic and adipic acid. Deuterated trifluoracetic acid was used for polyamide characterization. ^{1}H-NMR spectra in DMSO were recorded with 1.0 s of a relaxation delay, 4.09 s of an acquisition time, and 64 scans. The acquisition parameters for ^{13}C-NMR spectroscopy were a 90° pulse width, 1.0 s of a relaxation delay, 1.36 s of an acquisition time, and 1024 scans. Tetramethylsilane was used as a reference of 0 ppm.

LC-MS^n

Methyl muconate identification confirmation was performed on an Agilent 1100 high performance liquid chromatography (HPLC) system equipped with a diode array detector (DAD) and an Ion Trap SL (Agilent Technologies, Santa Clara, CA) MS with in-line atmospheric pressure chemical ionization (APCI). Each sample was injected at a volume of 25 μL into the LC-MS system. Compounds were separated using a Develosil C30 RPaqueous, 5 μm, 4.6 × 250 mm column (Phenomenex, Torrance, CA) at an oven temperature of 30°C. The chromatographic eluents consisted of A) water modified with 0.03% formic acid, and B) acetonitrile/water (9:1, v/v) also modified with 0.03% formic acid. At a flow rate of 0.7 mL/min, the eluent was a linear gradient starting at 100% A going to 70% A from 0-50 min, before equilibrium. Flow from the HPLC-DAD was directly routed in series to the APCI-MS ion trap. The DAD was used to monitor chromatography at 210 nm for a direct comparison to MS data. MS and MS^n parameters are as follows: smart parameter setting with target mass set to 165 Da, compound stability 70%, trap drive 50%, capillary at 3500 V, corona 20000 nA, fragmentation amplitude of 0.75 V with a 30 to 200 % ramped voltage implemented for 50 msec, and an isolation width of m/z 2 (He collision gas). The APCI nebulizer gas was set to 60 psi, with dry gas flow of 7 L/min held at 350 °C and a vaporizer temperature of 400°C. MS scans and precursor isolation-fragmentation scans were performed across the range of 40-500 Da.

HPLC quantification of metabolites

For quantification of cresols, methyl catechols, and 3-methyl muconate, culture supernatants were measured with HPLC on an Agilent1100 series system (Agilent USA, Santa Clara, CA) utilizing a Phenomenex Rezex RFQ-Fast Fruit H$^+$ column (Phenomenex, Torrance, CA) and cation H$^+$ guard cartridge (Bio-Rad Laboratories, Hercules, CA) at 85°C. A mobile phase of 0.01 N sulfuric acid was used at a flow rate of 1.0 mL/min and a diode array detector at 254 nm was used for compound detection. Products were identified by comparing the retention times and spectral profiles with pure compounds and were calculated based on a calibration curve generated for each compound. For comparisons of metabolite concentrations, a one mean, two-tailed Student's t-test was used unless otherwise stated.

Thermal and monomer purity characterization

Polymers, plasticizers, and monomers were characterized by differential scanning calorimetry (DSC) and thermogravimetric analysis (TGA). For DSC, all runs were conducted in an inert nitrogen environment at 10 °C/min. Monomers (e.g. 2-MM, 3-MM, 2-MA, and 3-MA) and plasticizers were tested for their melting point and purity by conducting a scan from -90 °C to 200 °C and the TA Universal Analysis software was used to calculate the purity via melting point depression. All polymers were tested for two cycles in which nylons were tested from -90 °C to 300 °C and PVC was tested from -90 °C to 100 °C. All data were reported as the result of the second heat. TGA was tested at a rate of 20 °C/min from room temperature to 900°C.

Cell culture and bioreactor cultivations

For shake flask experiments, strains were grown overnight from glycerol stocks in 5 mL of LB medium in a 14 mL culture tube, then resuspended in 1 mL M9 minimal medium (6.78 g/L disodium phosphate, 3 g/L monopotassium phosphate, 0.5 g/L NaCl, 1 g/L NH$_4$Cl, 2 mM MgSO$_4$ 100 μM CaCl$_2$, and 18 μM FeSO$_4$) supplemented with 20 mM glucose. The optical density at 600 nm (OD$_{600}$) of the resuspended cells was measured, and cells were inoculated immediately into shake flasks with an initial OD$_{600}$ of 0.1 unless otherwise stated. Shake flask experiments were performed using M9 minimal medium supplemented with 20 mM glucose and the specified concentrations of *m*-, *o*-, or *p*-cresol. Cultures were grown in 10 mL volumes in 50 mL baffled shake flasks and incubated at 30°C with shaking at 220 rpm. For comparisons of optical densities between strains and growth conditions, a one mean, two-tailed Student's t-test was used unless otherwise stated.

For bioreactor cultivations, seed cultures were initially grown overnight in LB. Next, cells were centrifuged and resuspended in M9 minimal medium supplemented with 20 mM glucose. 3 L bioreactors (Applikon) were inoculated with cells to an initial OD$_{600}$ of 0.2. The batch phase consisted of 1.2 L of M9 supplemented with 20 mM of glucose and initiated at a dissolved oxygen (DO) level of 100% and an agitation of 350 rpm. After 4 h, the cells were induced with 0.25 mM *m*- or *p*-cresol. When the glucose was depleted and the dissolved oxygen (DO) reached a level of 75%, the DO-stat fed-batch protocol was started. Feed bottles for the fed-batch phase contained 125 mM cresol, 900 mM glucose, and 35 g/L NH$_4$SO$_4$ that had been adjusted to a final pH of 7.0 with 4 N NaOH. Each feeding pulse was automatically activated each time the DO reached a value of 75% and aimed to feed 0.5 mM of cresol. Agitation was manually controlled to maintain DO levels between 20 and 75% (**Figure S10**). Bioreactors were sparged with air (1 vvm) and controlled at pH 7 by the addition of 4 N NaOH.

Preparation of 2-methyl muconic acid

2-methyl muconic acid was prepared from 3-methyl catechol according to previous articles.[6-8] To a mixture of acetic acid glacial (313 mg, 5.20 mM), 40% peracetic acid (900 mg, 4.73 mM) and ferric acetate (0.308 mg, 0.00161 mM), a solution of 3-methyl catechol (0.2g, 1.61 mM) in acetic acid (0.65 ml) was added dropwisely over a period of 1.0 hour using a syringe pump at ambient temperature. After the entire reaction solution was stirred for 20 hours, deionized H$_2$O (20 ml) was added. A white powder was precipitated. The solid precipitate was isolated by centrifugation (3500 rpm x 5 min), washed with cold di-H$_2$O (7 ml x 5 times) and dried in a vacuum oven at 40 °C for 24 hours to yield 29.5 mg of *trans,trans* -2-methyl muconic acid (11.7 %).

Preparation of 3-methyl muconic acid

3-Methyl muconic acid was prepared from 4-methyl catechol in the same manner of the 2-methyl muconic acid. To a mixture of acetic acid glacial (303 mg, 5.05 mM), 40% peracetic acid (872mg, 4.59 mM) and ferric acetate (3.5 mg, 0.0183 mM), a solution of 4-methyl catechol (0.2g, 1.53 mM) in acetic acid (0.65 ml) was added dropwisely over a period of 1.0 hour using a syringe pump at room temperature. After the reaction solution was stirred for 16 hours, deionized H$_2$O (20 ml) was added. A white precipitate generated was isolated by centrifugation (3500 rpm x 5 min), washed with cold deionized H$_2$O (7 ml x 5 times) and dried in a vacuum oven at 40 °C for 24 hours to yield 29.5 mg of *trans,trans*-3-methyl muconic acid (12.8 %).

Purification of methyl muconates from fermentation media

Muconates were separated and purified as previously described [9]. Briefly, the fermentation broth was initially treated with activated carbon at a concentration of 10 g/L to remove trace color compounds. The fermentation broth was subsequently rotovapped to remove excess water and concentrate the clarified culture broth. The broth was then acidified using sulfuric acid to a pH < 2, which caused the methyl muconic acid to crash out of solution as a solid white powder, which was subsequently dissolved in ethanol and filtered once more to remove any excess salts. After solvent removal, isomerically pure methyl muconic acids remained and they were used in subsequent transformations.

Polyamide synthesis

All polyamides were synthesized by the formation and subsequent melting of an amine-carboxylate salt at small scale (100-200 mg). To form the polyamide for a given carboxylic acid, both hexamethylene diamine (HMDA) and the carboxylic acids of interest were separately dissolved in 4 mL of water at a 0.25 M concentration. The HMDA and carboxylate solutions were subsequently combined while chilled and then the salt was precipitated by the addition of an excess of isopropanol. The salt was filtered and dried following precipitation. The salts were then loaded into a DSC pan and heated to 300°C to induce melting and polymerization. Following polymerization, thermal properties of the polymer melt were obtained. Samples were subsequently removed from the DSC pan and subject to TGA.

For the larger scale polymerizations or the modification studies, the same salt-based polymerization procedure was used but the scale was just increased to as much as 10 g. Proof-of-concept modification with thio-benzene were conducted by stirring the polymer in NMP over night with thiobenzene and reprecipitating the polymer with isopropanal. Films were prepared by dissolving the polyamides in trifluoracetic acid, casting, then letting the solvent evaporate.

Plasticizer synthesis

Plasticizers were synthesized by initially converting all four diacids to their acyl chloride by reflux in thionyl chloride with a catalytic amount of DMF. Following reflux, thionyl chloride was removed via vacuum distillation and compounds were purified via silica gel chromatography. The acyl chlorides were subsequently added to dichloromethane (DCM) with 2.1 equivalents of triethyl amine plus 2.1 equivalents of 2-ethyl hexanol. The reaction went to completion and the plasticizers were separated out via silica gel chromatography to yield oils that were clear or slightly yellow.

Additionally, to reduce reliance on stoichiometric equivalents, namely thionyl chloride, a later proof of concept was conducted in which the acids were refluxed in toluene with 2 equivalents of 2-ethyl hexanol and 1 wt. % *p*-tsOH as a catalyst. After silica gel chromatography, oils that were clear or slightly yellow were still obtained at yields varying from 82% to 98%. Specifically, the methyl muconates possess lower yields due to possible solubility issues.

Toxicity predictions from EPA tools

Toxicity predictions were obtained from the EPA Toxicity Estimation Software Tool (TEST)[10] and the human metabolism and environmental breakdown products were estimated with the EPA Chemical Transformation Simulator (CTS).[11] We created in-house scripts in Python to allow high-throughput workflow and analysis.
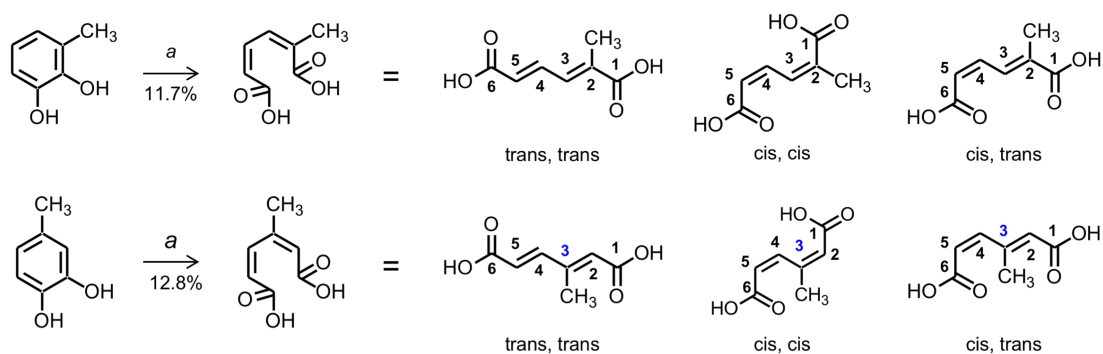
Figure S1. Reaction scheme for chemical synthesis of 2- and 3-methyl muconic acid. For both schemes, "a" indicates AcOH/ AcOOH/ Fe(OAc)₂OH/rt/16 hrs. See Supplementary Materials and Methods for more information on chemical synthesis.
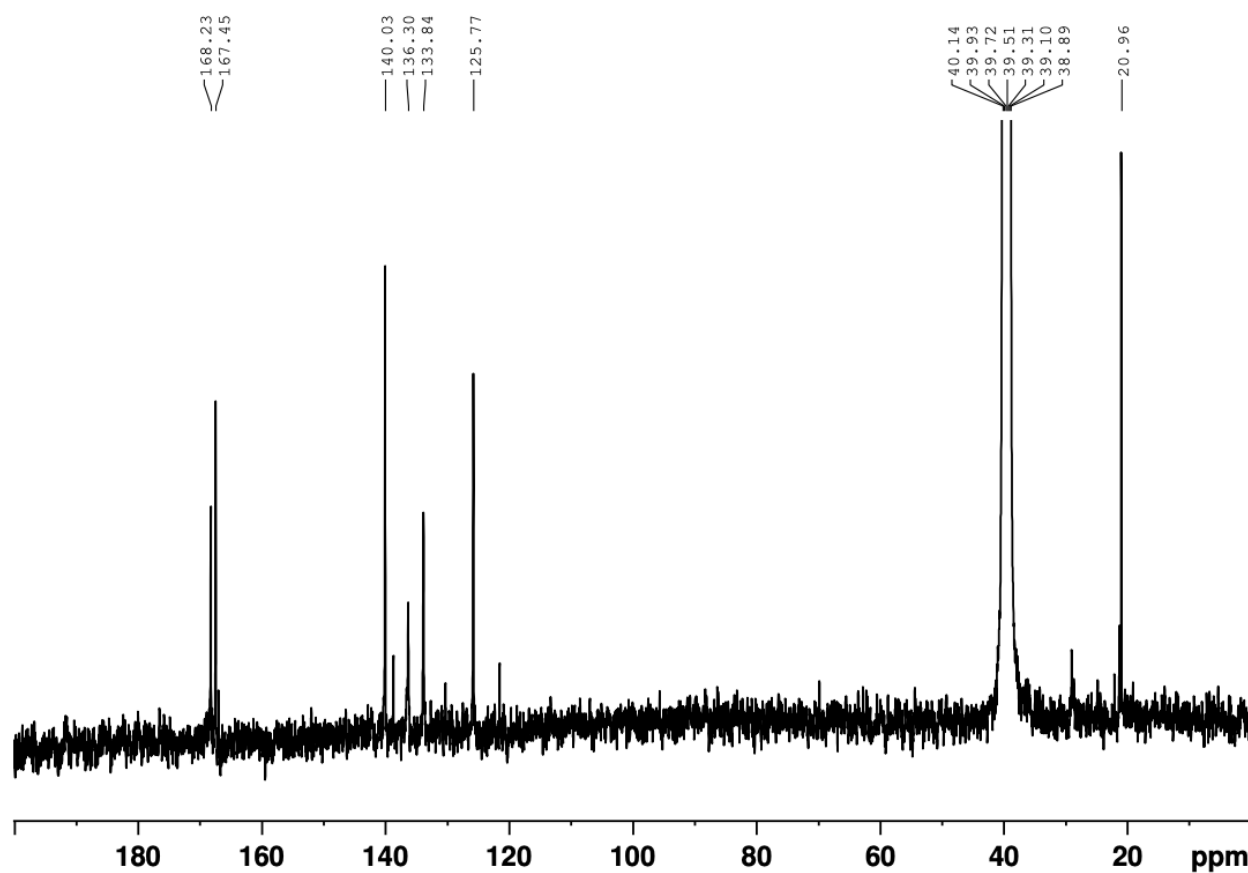
Figure S2. ^{13}C-NMR of chemically synthesized 2-methyl muconic acid in DMSO-d_6. ^{13}C NMR (100 MHz, DMSO-d_6) 168.2, 167.4, 140.0, 136.3, 133.8, 125.8, 20.9 ppm.
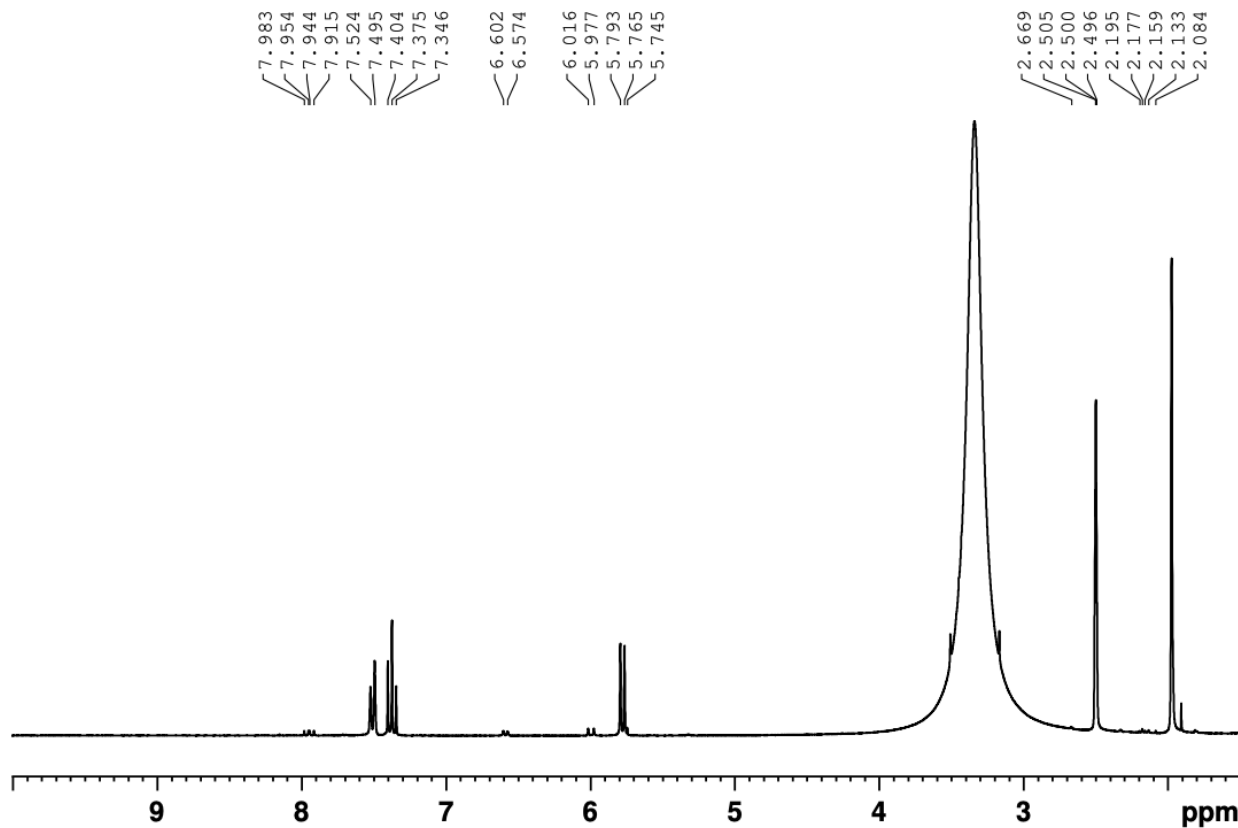
Figure S3. ^{1}H-NMR of chemically synthesized 2-methyl muconic acid in DMSO-d_6. ^{1}H NMR (400 MHz, DMSO-d_6) δ 7.51 (1H, d, J=11.6Hz, H3), 7.38 (1H, t, J=11.6Hz, H4), 5.78 (1H, d, J=11.4Hz, H5), 1.97 (3H, s, CH$_3$).
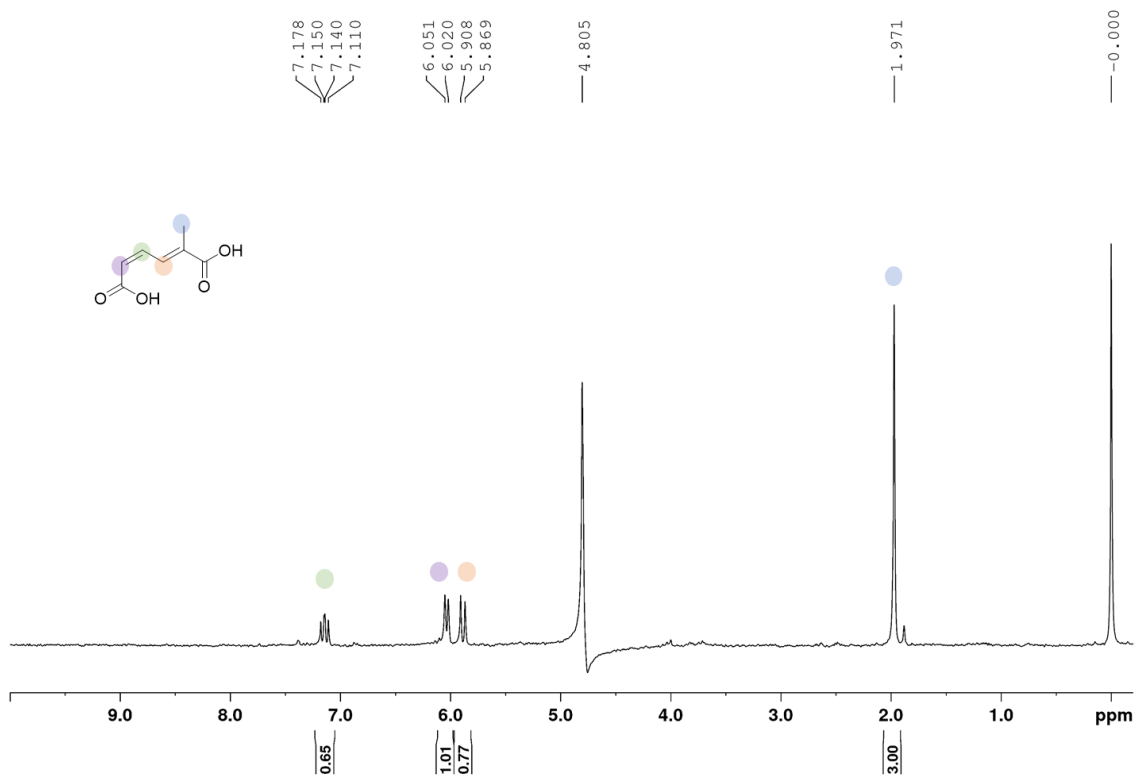
Figure S4. ¹H NMR of 2-methyl-*cis,trans*-muconic acid synthesized chemically from the oxidative ring cleavage of 3-methyl catechol in D₂O. ¹H NMR (400 MHz, D₂O, δ): 7.18-7.11 (dd, 1H, J= 11.2Hz and 12.0Hz), 6.03 (d, 1H, J= 12.4Hz), 5.88 (d, 1H, J= 15.6Hz), 1.97 (s, 3H), COO*H* not observed in D₂O.
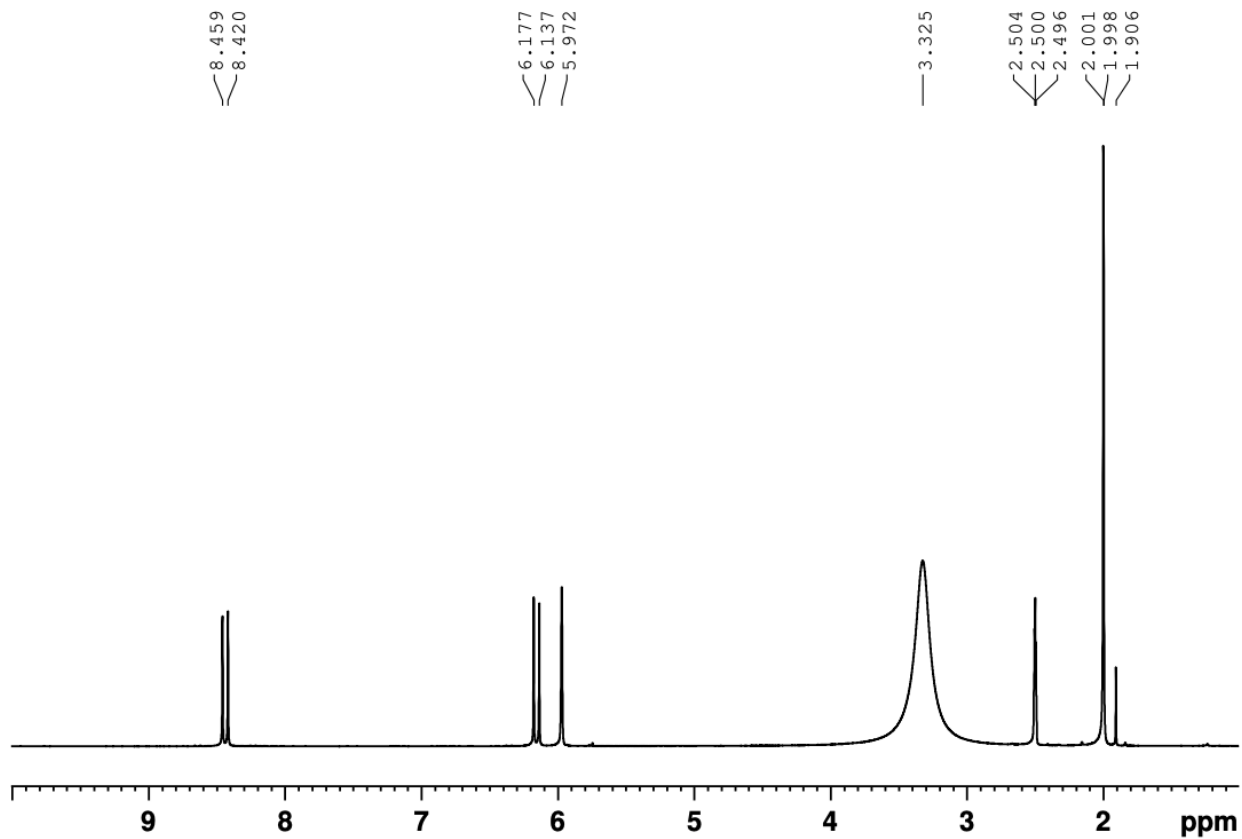
Figure S5. ^{1}H-NMR of chemically synthesized 3-methyl muconic acid in DMSO-d_6. ^{1}H NMR (400 MHz, DMSO-d_6) δ 8.44 (1H, d, J=16Hz, H4), 6.18 (1H, d, J=16Hz, H5), 5.97 (1H, d, H2), 2.00 (3H, s, CH$_3$).
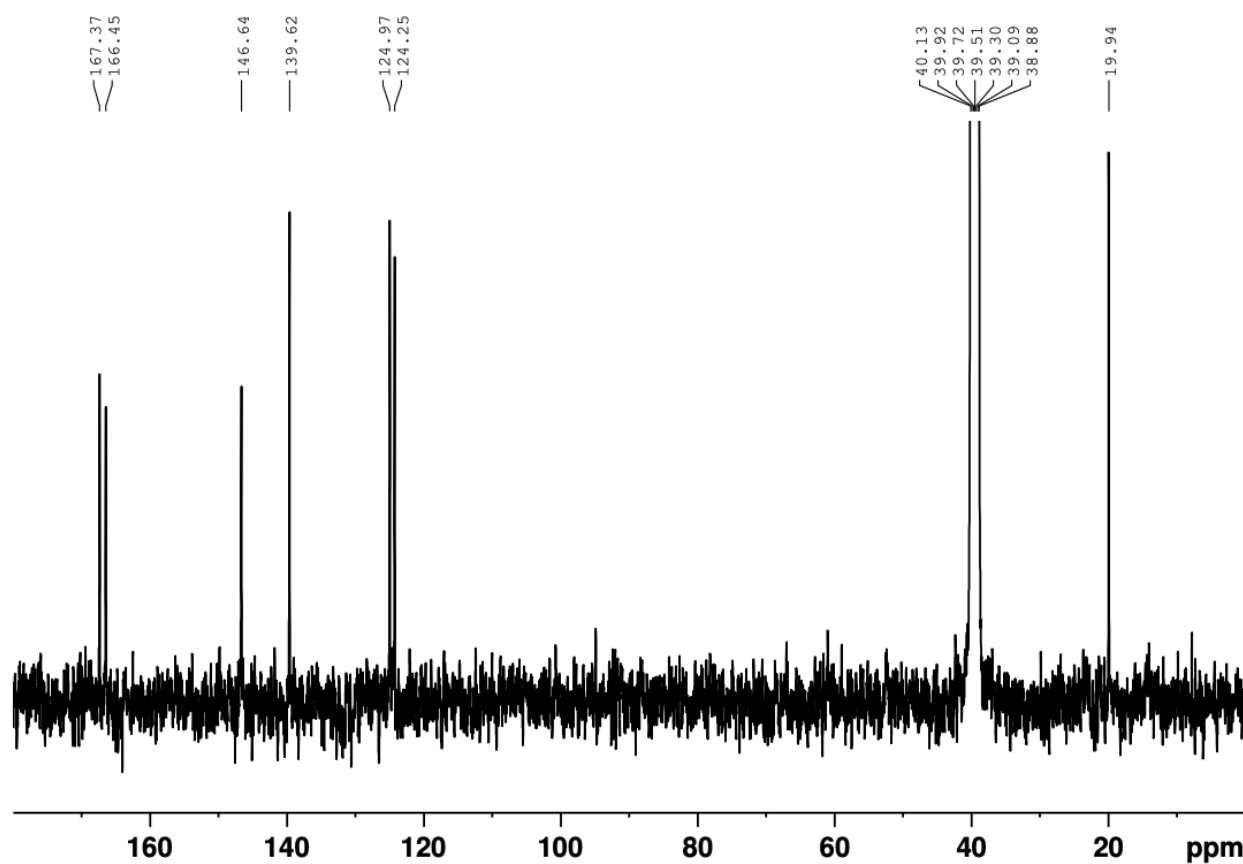
Figure S6. ^{13}C-NMR of chemically synthesized 3-methyl muconic acid in DMSO-d_6. ^{13}C NMR (100 MHz, DMSO-d_6) 167.4, 166.5, 146.6, 139.6, 125.0, 124.2, 19.9 ppm.
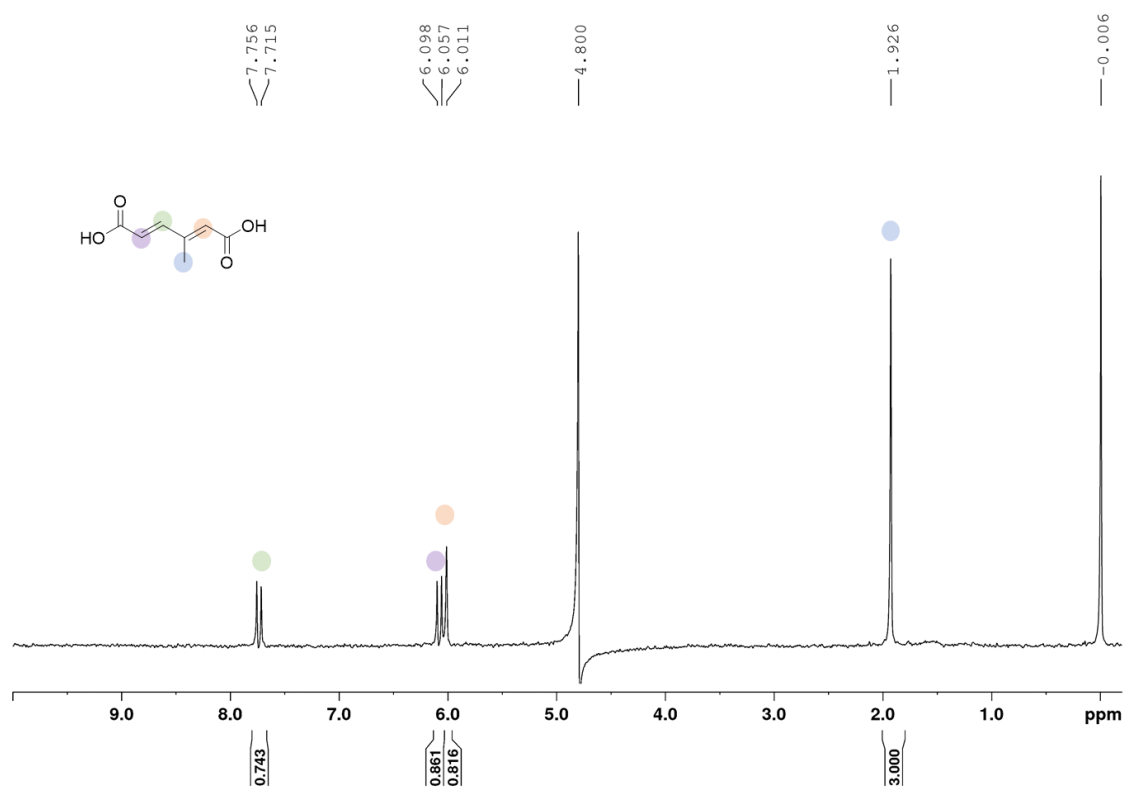
Figure S7. ¹H NMR of 3-methyl-*trans,trans*-muconic acid synthesized chemically from the oxidative ring cleavage of 4-methyl catechol in D₂O. ¹H NMR (400 MHz, D₂O, δ): 7.73 (d, 1H, J= 16.4Hz), 6.07 (d, 1H, J= 16.4Hz), 6.01 (s, 1H), 1.93 (s, 3H), COO*H* not observed in D₂O
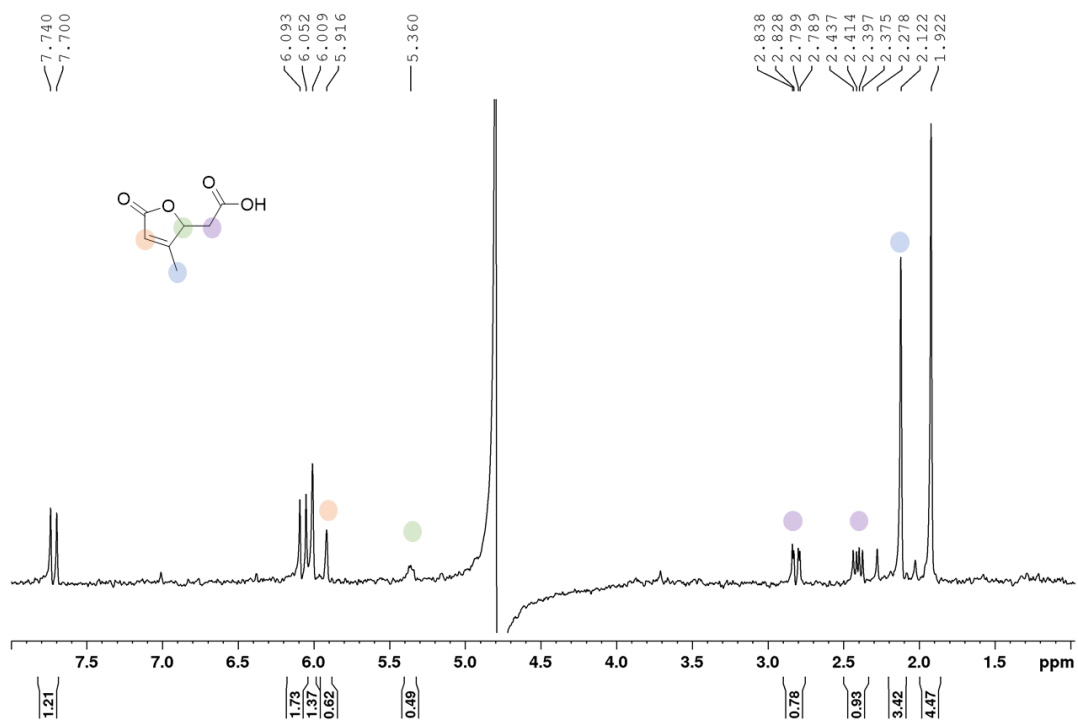
Figure S8. ^{1}H NMR spectra of *p*-cresol shake flask growth experiment taken at 36 hours in D$_2$O. The mixture of 3-methyl-*trans,trans*-muconate and 2-(3-methyl-5-oxo-2H-furan-2-yl)acetic acid (3-methyl muconolactone).
^{1}H NMR of 3-methyl-*trans,trans*-muconate (400 MHz, D$_2$O, δ): 7.73 (d, 1H, J= 16.4Hz), 6.07 (d, 1H, J= 16.4Hz), 6.01 (s, 1H), 1.93 (s, 3H), COO*H* not observed in D$_2$O. ^{1}H NMR of 2-(3-methyl-5-oxo-2H-furan-2-yl)acetic acid (400 MHz, D$_2$O, δ): 5.92 (s, 1H), 5.36 (m, 1H), 2.80 (dd, 1H, J=15.6, 4.0 Hz), 2.40 (dd, 1H, J= 14.5, 8.9 Hz), 2.12 (s, 1H).
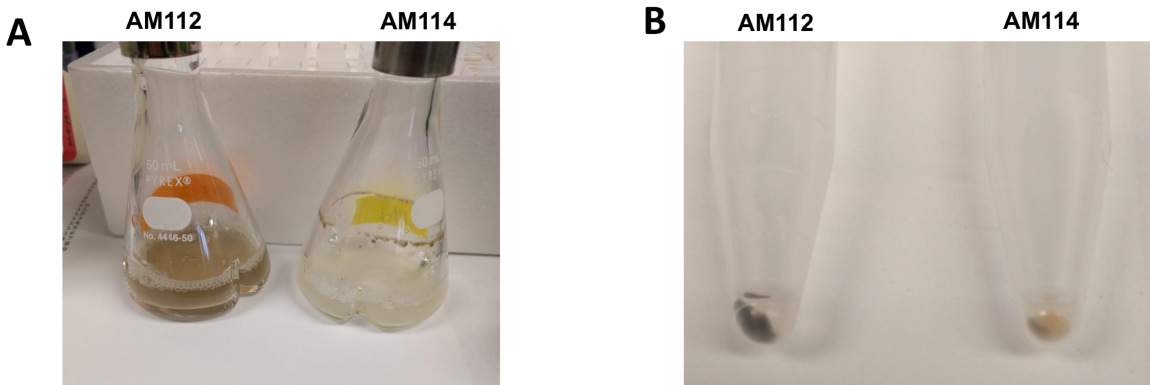
Figure S9. Reduced darkening of cultures for AM114 during shake flask cultivations. A. Shake flasks of AM112 and AM114 after 36 hours with 3.2 mM *o*-cresol. **B.** Cell pellets exhibiting a dark color, suggesting a potential loss of carbon from oxidation of 3-methyl catechol.
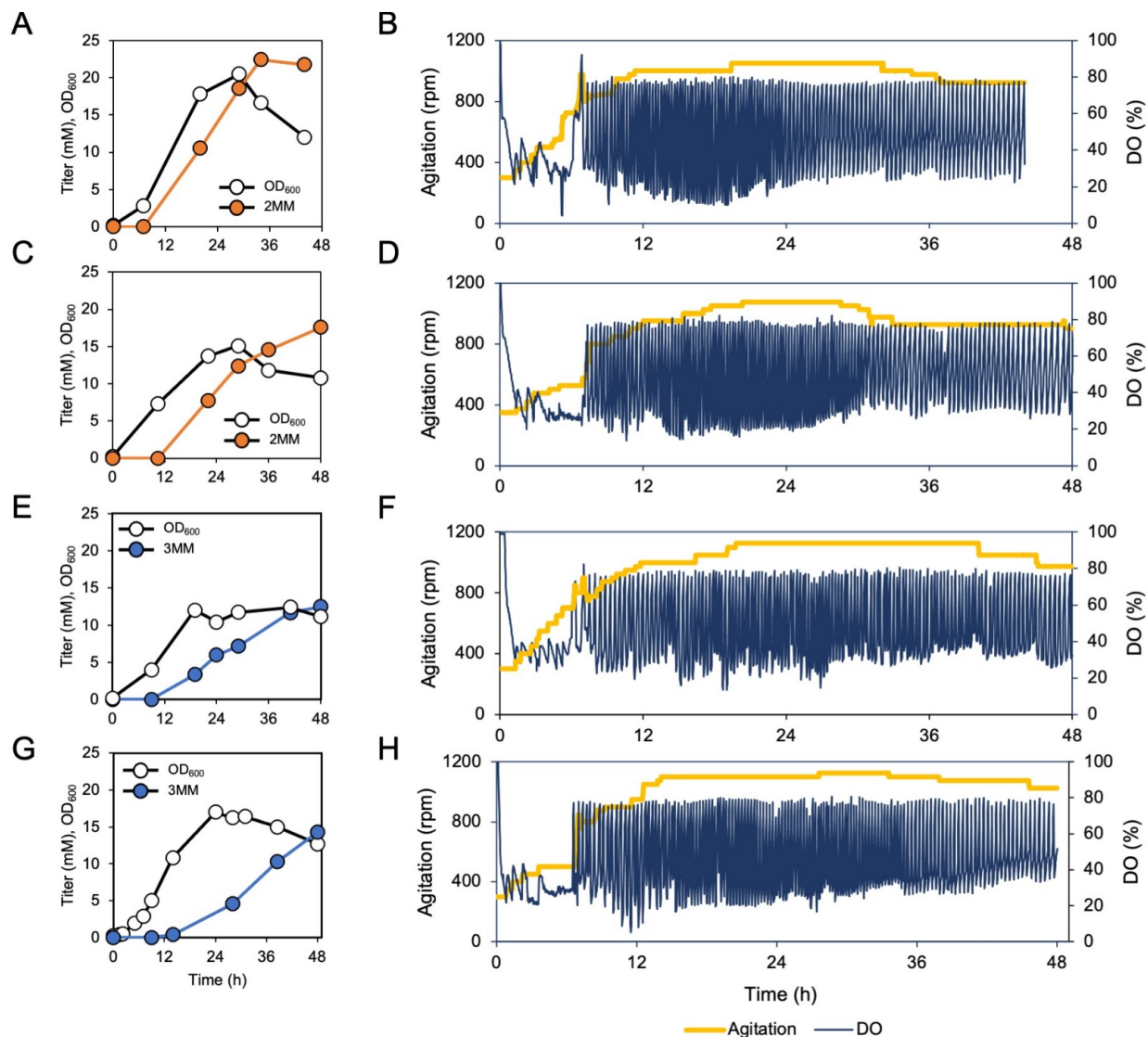
Figure S10. Individual bioreactor cultivations for 2-methyl muconic acid and 3-methyl muconic acid production with dissolved oxygen (DO) and agitation profiles. A, B. Bioreactor run #1 with AM114 feeding *m*-cresol to produce 2-methyl muconic acid (2MM). **C, D.** Bioreactor run #2 with AM114 feeding *m*-cresol to produce 2MM. **E,F.** Bioreactor run #1 feeding *p*-cresol to produce 3-methyl muconic acid (3MM). **G, H.** Bioreactor run #2 feeding *p*-cresol to produce 3MM.
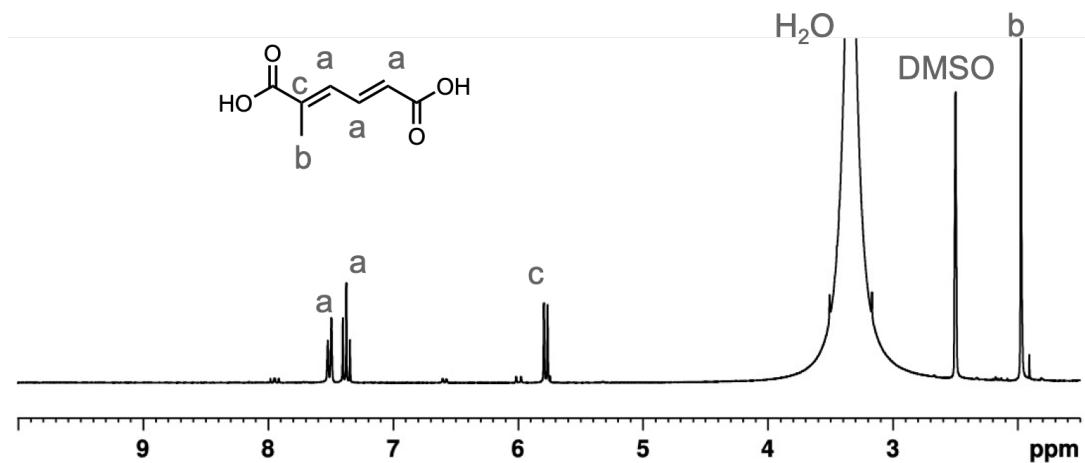
Figure S11. ¹H-NMR of 2-methyl muconic acid post-fermentation separation in DMSO-d_6. Peak assignments are labeled. Large water peak is cropped.
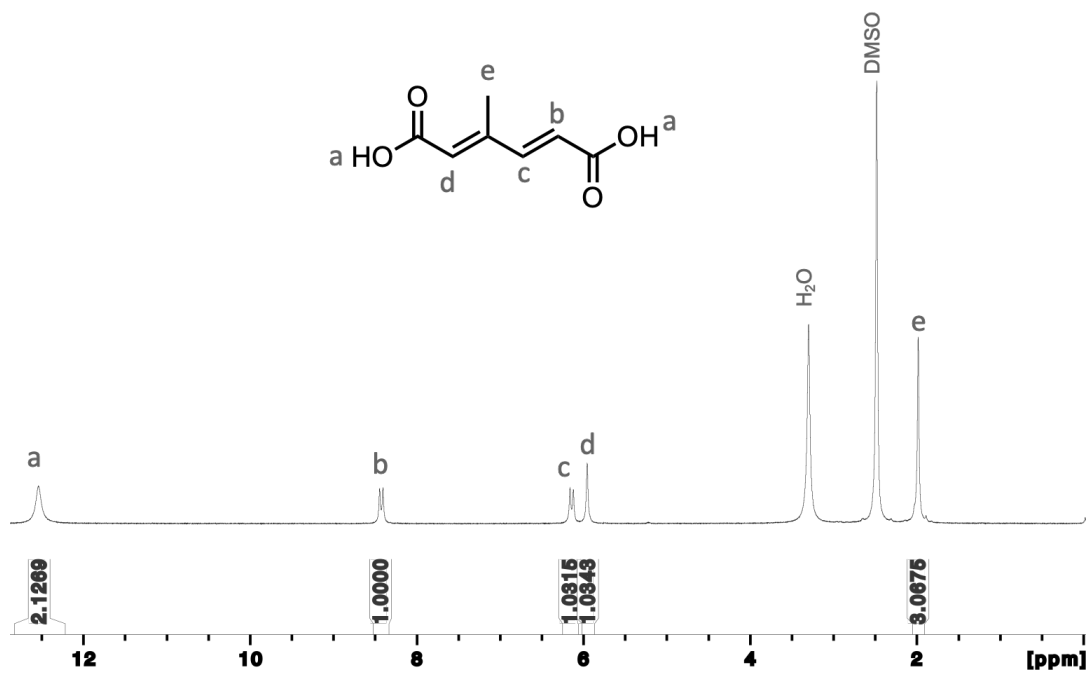
Figure S12. ¹H-NMR of 3-methyl muconic acid post-fermentation separation in DMSO-*d₆*. Peak assignments are labeled.
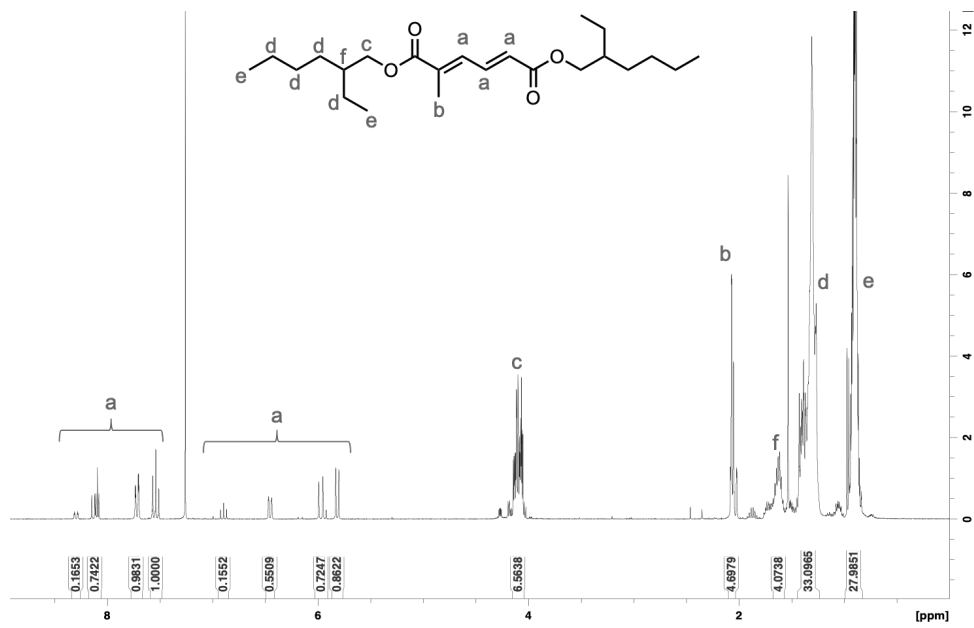
Figure S13. ¹H-NMR of 2-methyl muconic acid-based plasticizer. Peak assignments are labeled.
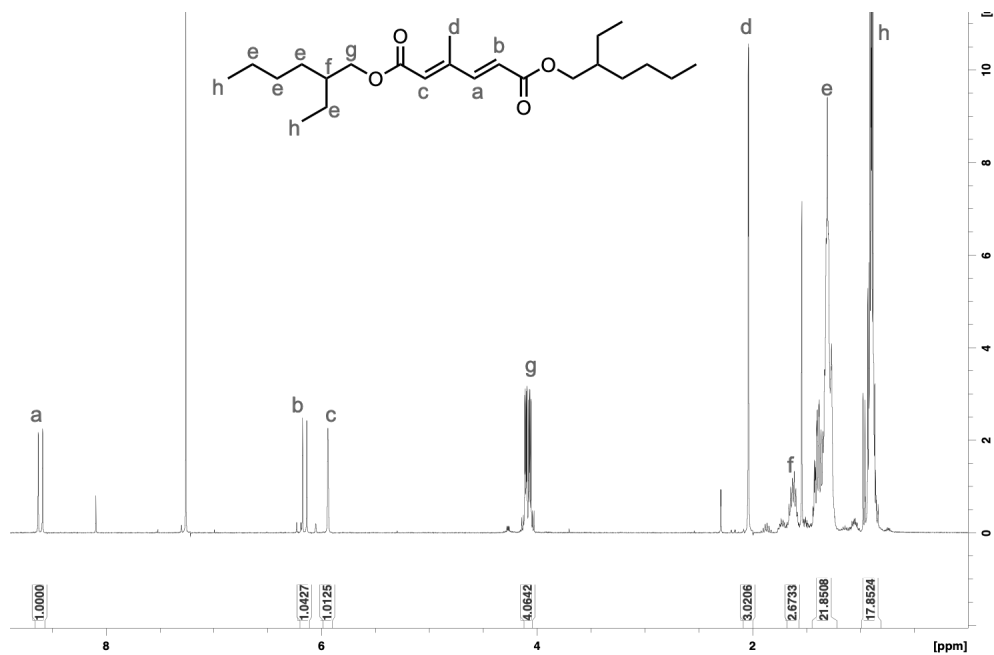
Figure S14. ¹H-NMR of 3-methyl muconic acid-based plasticizer. Peak assignments are labeled.
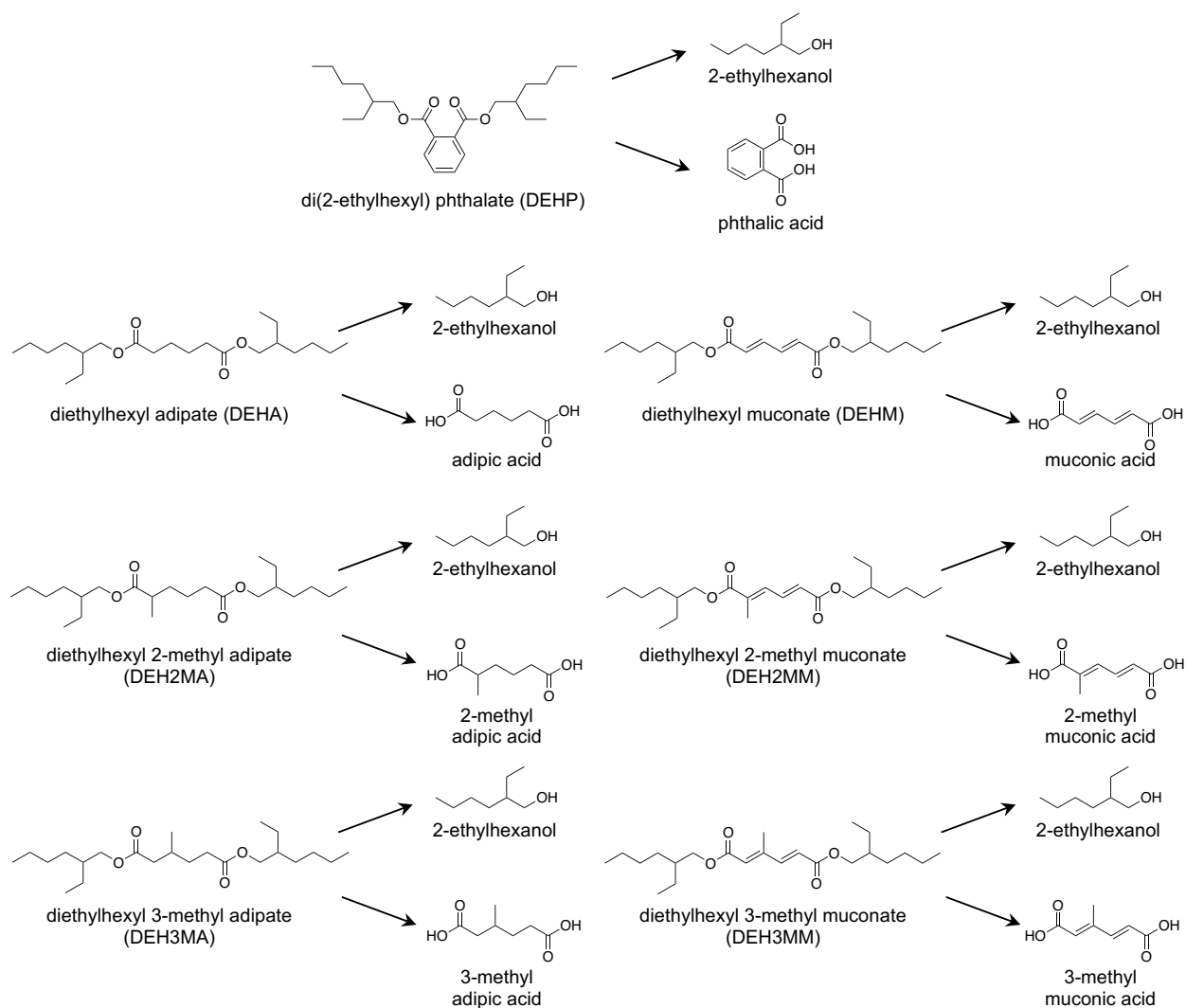
Figure S15. Predicted metabolic and environmental transformations of plasticizers. All plasticizers in this study were predicted by the EPA Chemical Transformation System to hydrolyse back to their component diacids and alcohols, both in the environment via abiotic hydrolysis and metabolized by humans. Toxicity predictions for these compounds in blue are provided in **Table S7**. None of these compounds were predicted to further react in the environment via abiotic means, while 2-ethylhexanol and all diacids except for phthalic acid were predicted to be further metabolized in humans (**Figure S16**).
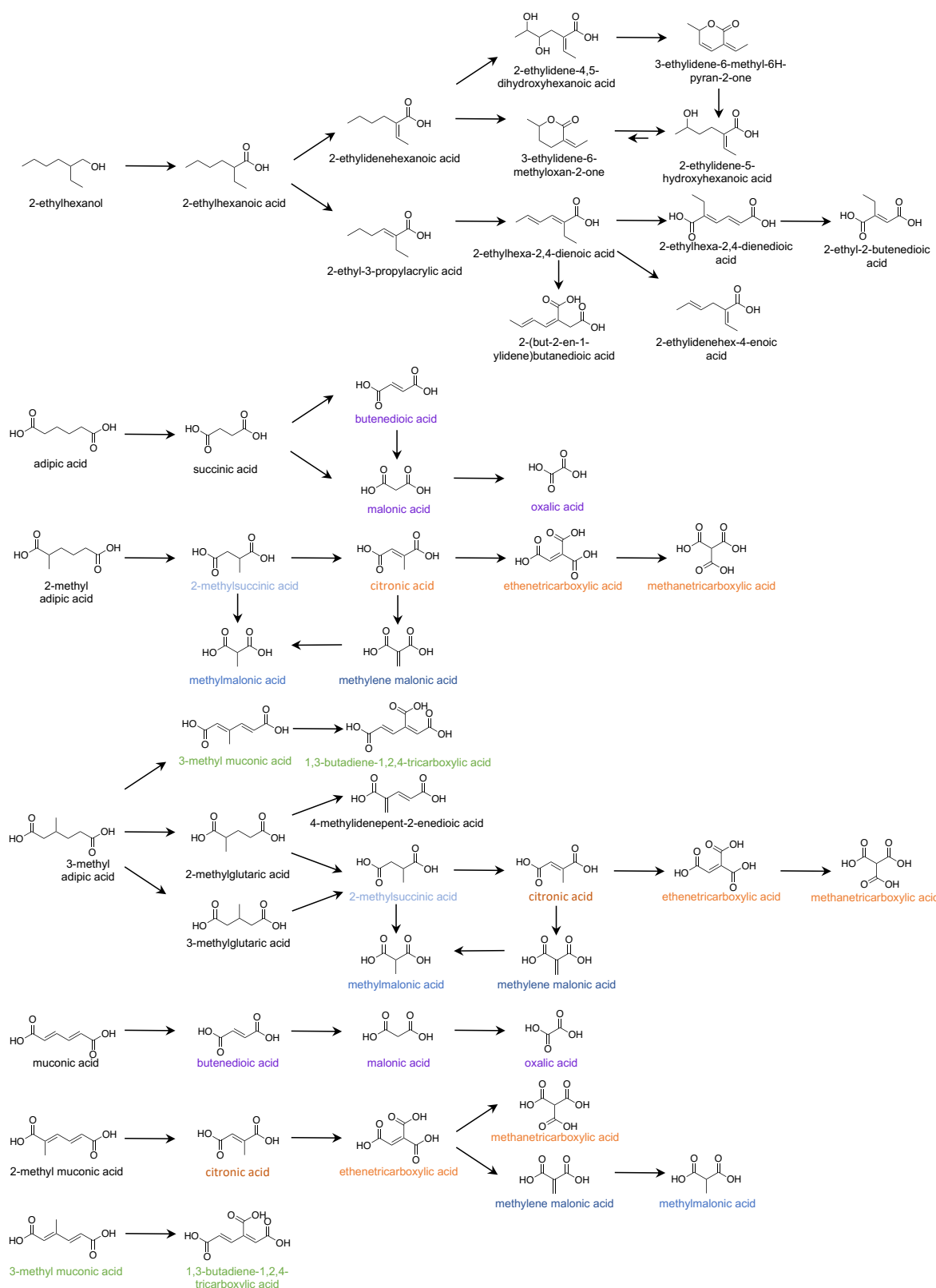
Figure S16. Predicted metabolites from 2-ethylhexanol and diacids. Main metabolic pathways predicted by the EPA Chemical Transformation System. Color used to highlight metabolites common to multiple diacids.

Table S1. Strains and plasmids used in this study.

Strain	Genotype	Strain information
Pseudomonas putida KT2440		ATCC 47054.
P. putida CF600		Gift from Victoria Shingler, Department of Molecular Biology, Umeå University
AM107	*P. putida* KT2440 Δ*catBC*::Ptac:*dmpKLMNOP*:*catA*	*catBC* was replaced in KT2440 with Ptac:*dmpKLMNOP*:*catA* using pAM011 and this gene replacement was confirmed by diagnostic colony PCR amplification of a 7747 bp product with primer pair oCJ086/oCJ087.
AM111	*P. putida* KT2440 Δ*catBCA*::Ptac:*dmpKLMNOP*:*clcA*	*catBCA* was replaced in KT2440 with Ptac:*dmpKLMNOP*:*clcA* using pAM012 and this gene replacement was confirmed by diagnostic colony PCR amplification of a 7715 bp product with primer pair oCJ086/oCJ087.
AM112	*P. putida* KT2440 Δ*catBC*::Ptac:*dmpKLMNOP*:*catA* Δ*catA2*	*catA2* was deleted from AM107 using pCJ004 and this deletion was confirmed by diagnostic colony PCR amplification of a 2089 bp product with primer pair oCJ084/oCJ085.
AM114	*P. putida* KT2440 Δ*catBCA*::Ptac:*dmpKLMNOP*:*clcA* Δ*catA2*	*catA2* was deleted from AM111 using pCJ004 and this deletion was confirmed by diagnostic colony PCR amplification of a 2089 bp product with primer pair oCJ084/oCJ085.

Plasmid Name	Use	Plasmid construction details
pBTL-2	Episomal expression in *P. putida* KT2440	Addgene plasmid # 22806. Previously described in Prior *et al.*, 2010.[12]
pK18sB	Genomic integration into *P. putida*. Contains Kanamycin resistance cassette for selection and *sacB* for counterselection.	Genbank # MH166772, Addgene Plasmid # 177838. Construction details of pK18sB are described in Jayakody, *et al.*, 2018[1]
pCJ004	Deletion of *catA2* in *P. putida* KT2440	Construction details of pCJ004 are described in Johnson and Beckham, 2015[2]
pCJ005	Replacement of *catBCA* with Ptac:*xylE* (from *P. putida* mt-2) in *P. putida* KT2440	Construction details of pCJ004 are described in Johnson *et al.*, 2019[13]
pCJ106	Replacing *catBCA* with *xylE* (from *P. putida* mt-2) in *P. putida* KT2440	The Δ*catBCA*::*xylE* cassette (3092 bp) was amplified from pCJ005 with oCJ542/oCJ545 and assembled into pK18sB digested with EcoRI and HindII. Plasmid was confirmed by diagnostic digest with KpnI and by Sanger sequencing.
pAM006	Integration of Ptac:*dmpKLMNOPQBCDEFGHI* from *P. putida* CF600 in place of *catBCA*	*dmpKLMNOPQBCDEFGHI* was amplified from *P. putida* CF600 genomic DNA using the primer pair oAM25/oAM022 (12303 bp). An additional primer pair of oAM026/oAM024 was used to amplify pCJ106 which was previously designed for integration of *xylE* in place of *catBCA* (5125 bp). These fragments were then assembled together using Gibson Assembly (17331 bp). Sanger sequencing was used to confirm the correct sequencing using oAM33-oAM60.
pAM008	Episomal expression of *clcA* in *P. putida* KT2440	*clcA* from *R. opacus* 1CP was codon optimized for *P. putida* KT2440 and synthesized as a gBlock by IDT. pBTL-2 was amplified using primers oCJ160/oCJ161 and these two fragments were assembled using Gibson Assembly (3381 bp).
pAM011	Replacing *catBC* with Ptac:*dmpKLMNOP*:*catA* in *P. putida* KT2440	The *dmpKLMNOP* cluster from *P. putida* CF600, upstream targeting region, and pK18sB backbone were amplified from pAM006 using the primer pair oAM093/oAM094 (8747 bp). The downstream targeting region, *catA*, was cloned from genomic KT2440 genomic DNA using oAM95/oAM96 (993 bp). These fragments were then assembled together using Gibson Assembly (9693 bp).
pAM012	Replacing *catBCA* with Ptac:*dmpKLMNOP*:*clcA* in *P. putida* KT2440	The *dmpKLMNOP* cluster from *P. putida* CF600, downsteam and upstream homology regions, and pK18sB backbone were amplified from pAM006 using oAM90/oAM91 (9877 bp). *clcA* was amplified from pAM008 using the primer pair oAM088/oAM089 (834 bp). These fragments were then assembled together using Gibson Assembly (10661 bp).

Table S2. DNA oligos used in this study.

Primer	Sequence (5' to 3')
oCJ084	CCTCAATGGCTTTGCCAG
oCJ085	GTACAACACACTGCCAGC
oCJ086	TGTGGGCATGGTGTGTTC
oCJ087	TCTTCAAAGCGTCCGGTG
oCJ160	GATATCATTCAGGACGAGCCTCAGACTCC
oCJ161	CTCTAGAGTGTGAAATTGTTATCCGCTCACAATTCC
oCJ542	AGGAAACAGCTATGACATGATTACGAATTCCCTGTTGCTCGATCAACGCCAG
oCJ545	CGTTGTAAAACGACGGCCAGTGCCAAGCTTCGCCTGCTCCAGGTTGAATGC
oAM22	TCACAGTGACATAACCTCGAACGCGGCCGCAAAAAGTGCCTCCTGCCACAGAG
oAM23	AGTCAAAAGCCTCCGGTCGGAGGCTTTTGACTTGTTGCCAGGTCCCGTCA
oAM24	AGTGCCCCTCTGTGGCAGGAGGCACTTTTTGCGGCCGCGTTCGAGGTTATG
oAM25	AATTTCACACTCTAGAGGCGTAGAGAATAGATGACCGTGACCAATACCCCCA
oAM26	CGGTCATCTATTCTCTACGCCTCTAGAGTGTGAAATTGTTATCCGCTCACAATTCCACAC
oAM33	TGTTTTCAGACCTTGGCACA
oAM34	ATTGGCACAAGGTCACCG
oAM35	GCTTGCCGAAAATGACGCTA
oAM36	ATCAAGATCACCGACTGGGA
oAM37	GAAGTGATCAAGTTCATGCTCG
oAM38	AAGAACGAGCCGGTGAAGTA
oAM39	AAGCATGCTGCGTCTGAAC
oAM40	ACAAGCAACTGAAAGTCGGC
oAM41	GACCAGTCGGTGCTCAGTG
oAM42	CCGTCCGGACACTTTTTC
oAM43	CTCGCCTTTTTGCAGAGATT
oAM44	TCAACGCCATCACCTTCAC
oAM45	GGACCGAGAACACCTCGC
oAM46	GTCAGCTTCCCGATCACC
oAM47	ATGCTCGAACGCCGACTG
oAM48	CGTCGACATCGGCGGTAT
oAM49	AGCAAAGCCATCGAAGTGAT
oAM50	GGACGGCACACTGACCTG
oAM51	TCTACACCCTGATGGATGC
oAM52	TCACCAAGGCTCCATTGCA
oAM53	GGTGCGTGTGCTCATTACC
oAM54	TCATCTTGAAGAAGTACCGTCG
oAM55	AACCTGGAGCAGGCGAAG
oAM56	AAGAGCATCAGGGGCTCG
oAM57	GGCACTGTCGCAAACTATCA
oAM58	CAAAAACTTCTGCAAAGCGA
oAM59	GCATCCTTGAACAAGGACAA
oAM60	CAATGGACGAAGCGATGG
oAM088	TTCGGCCCTGTTCAAGCGCATCTGAGGAGGACAAGATGGCTAACACTCGCGTAATC
oAM089	AAACTCTTTAACGAACACTCTCATACTAGTTGTGCTGCAGGATGAA
oAM090	TATGAGAGTGTTCGTTAAAGAGTTTGATTTGAATCC
oAM091	TCAGATGCGCTTGAACAGGG
oAM092	CGACAACTTCTTCGACAGCG
oAM093	TCAGATGCGCTTGAACAGGGC
oAM094	AAGCTTGGCACTGGCCGTC
oAM095	CCCTGTTCAAGCGCATCTGAGGAGGACAAGATGACCGTGAAAATTTCCCACACTGC
oAM096	TGTAAAACGACGGCCAGTGCCAAGCTTTCAGCCCTCCTGCAACGC

Table S3. Synthesized DNA sequence for construction of pAM008 with codon optimized *clcA* from *R. opacus* 1CP. Bold indicates start and stop codons of gene, green indicates overlaps for assembly into the pBTL2 vector, and red indicates designed RBS using the RBS calculator.[3]

gtgagcggataacaatttcacactctagag**aacaaggtatcc**ATGGCTAACACTCGCGTAATCGAGCTCTTCGACGAATTCACC
GATCTTATTCGTGACTTCATTGTCCGTCACGAAATCACCACCCCCGAGTACGAAACCATCATGCAGTACATGATCTCGGTTGGC
GAGGCTGGCGAGTGGCCGCTGTGGCTGGACGCTTTCTTTGAAACCACCGTCGACAGCGTGAGCTACGGCAAGGGCAACTGGACC
TCGAGCGCGATCCAGGGCCCTTTCTTCAAGGAGGGCGCCCCTCTGCTGACCGGCAAGCCGGCGACCCTGCCGATGCGTGCCGAC
GAGCCTGGTGACCGCATGCGCTTCACCGGCAGCGTTCGCGACACCTCGGGCACCCCTATTACCGGCGCCGTGATTGACGTGTGG
CACTCTACCAACGATGGCAACTACAGCTTTTTTCAGCCCGGCCTTGCCGGACCAGTACCTCCTGCGTGGTCGAGTGGTGCCGGCA
GAAGACGGCTCGATCGAATTCCACAGCATCCGCCCGGTTCCCTACGAGATCCCGAAAGCTGGCCCAACCGGCCAGCTGATGAAC
TCCTACCTGGGCCGTCACAGCTGGCGCCCGGCTCACATCCACATCCGCATCACCGCCGACGGTTACCGCCCGCTCATCACCCAG
CTGTACTTCGAAGGCGACCCTTATTTGGACTCGGACTCGTGCTCGGCTGTCAAAAGCGAACTGGTCCTGCCGGTCAACAAGATC
GACATTGACGGCGAAACCTGGCAGCTGGTCGACTTCAACTTCATCCTGCAGCACAAC**TAG**gatatcattcaggacgagcctcag
actcca

Table S4. Supplementary Excel file with raw biological data and processing information for metabolite quantification using ^{1}H-NMR.

Tab 1. Cover sheet.
Tab 2. Raw data of OD_{600} and metabolite concentrations from shake flask experiments shown in Figures 2, 4, and 5.
Tab 3. Raw data for analysis of NMR files for quantification of 2-methyl muconic acid from *m*-cresol shake flask experiments shown in Figures 2 and 5.
Tab 4. Raw data for analysis of NMR files for quantification of 2-methyl muconic acid from *o*-cresol shake flask experiments shown in Figures 2 and 5.
Tab 5. Raw data for analysis of NMR files for quantification of 3-methyl muconolactone from *p*-cresol shake flask experiments and single bioreactor run feeding *p*-cresol.
Tab 6. Raw data for OD_{600}, methyl muconic acid concentrations, dissolved oxygen, and agitation speed for individual bioreactor runs shown in Figure 6 and S10.

Table S5. Methyl muconic acid cultivations in bioreactor for subsequent product isolation. The table shows product titers, yields, and absolute amount in the bioreactors at two different time points. The table also includes the absolute amount of isolated product from each bioreactor and the product recovery yield.

Reactor Label	Titer (g/L)	Yield (mM/mM)	Absolute Amount (g)	Time (h)	Titer* (g/L)	Yield* (mM/mM)	Absolute Amount* (g)	Time* (h)	Isolated Product (g)	Product recovery yield (%)
2-Methyl Muconic Acid										
2MM-1	1.87	0.29	3.38	44.00	2.78	0.35	5.70	98.00	3.1	54.43
2MM-2	2.75	0.40	5.12	48.00	3.67	0.48	7.40	100.00	4.4	59.50
3-Methyl Muconic Acid										
3MM-1	2.23	0.32	4.21	48.00	2.64	0.31	5.63	79.00	3.8	67.46
3MM-2	1.94	0.29	3.62	49.00	1.94	0.28	3.67	51.00	3.2	87.17

* Time point at which bioreactors were harvested for further product isolation.

Table S6. Monomer melting temperatures and purity as determined by differential scanning calorimetry.

Chemical	Melting Temperature T_m (°C)	Std. Dev. (°C)	Purity, (mol %)	Std. Dev. (%)
Synthesized Standards				
2-Methyl Muconic Acid	108	± 5	99.3	±0 .7
3-Methyl Muconic Acid	111.5	± 5	99.5	±0 .7
2-Methyl Adipic Acid	89.3	± 5	99.7	±0 .7
3-Methyl Adipic Acid	92.1	± 5	99.5	±0 .7
Bio-derived Molecules Post Separations				
2-Methyl Muconic Acid	108	± 5	99.2	±0 .7
3-Methyl Muconic Acid	109.7	± 5	98.1	±0 .7
2-Methyl Adipic Acid	88.1	± 5	98.7	±0 .7
3-Methyl Adipic Acid	91.9	± 5	99.0	±0 .7

Note: The plasticizers do not exhibit melting/freezing behaviour in the range of -90 °C to 200 °C.

Table S7. Thermal data for all nylons synthesized from the polymerization of the listed diacid with hexamethylene diamine. All results across a set of three plus synthesized polymers are within instrument noise for the given measurement. This table includes the tabular data for **Main Text Figure 7A** and **7C** as well as data not included in that figure for the alternate isomers and control reactions with non-bio-derived methyl muconates.

Diacid	Glass Transition Temperature, T_g (°C)	Std. Dev. (°C)	Melting Temperature, T_m (°C)	Std. Dev. (°C)	Decomposition Temperature, $T_{D,5}$ (°C)	Std. Dev. (°C)
Adipic Acid	62	± 3	262	± 5	320	± 10
3-Methyl Adipic Acid	43	± 3	230	± 5	297	± 10
2-Methyl Adipic Acid	39	± 3	232	± 5	292	± 10
2-Methyl Adipic/3-Methyl Adipic (50/50 Molar Blend)	41	± 3	229	± 5	311	± 10
Adipic/2-Methyl Adipic/3-Methyl Adipic (50/25/25 Molar Blend)	62	± 3	237	± 5	320	± 10
trans,trans -Muconic Acid	42	± 3	203	± 5	293	± 10
3-Methyl Muconic Acid	-43	± 3	137	± 5	250	± 10
2-Methyl Muconic Acid	-45	± 3	143	± 5	251	± 10
2-Methyl Muconic/3-Methyl Muconic (50/50 Molar Blend)	-41	± 3	141	± 5	250	± 10
Non-Bio-derived Standard Control Reaction: 2-Methyl Muconic/3-Methyl Muconic (50/50 Molar Blend)	-39	± 3	147	± 5	246	± 10
Adipic/2-Methyl Muconic/3-Methyl Muconic (50/25/25 Molar Blend)	43	± 3	232	± 5	283	± 10
Thiobenzene Modified Adipic/2-Methyl Muconic/3-Methyl Muconic (50/25/25 Molar Blend)	41	± 3	197	± 5	403	± 10
Thiobenzene Modified *trans,trans* -Muconic Acid	46	± 3	196	± 5	407	± 10

Table S8. Tabular data for **Figure 7B**. Standard deviation is based off instrument error and fluctuations for the given sample.

Diacid	Water Permeability $(g*mm)/(m^2*day)$	Std. Dev. $(g*mm)/(m^2*day)$
Adipic Acid	1.01	± 0.05
2-Methyl Adipic/3-Methyl Adipic (50/50 Molar Blend)	0.89	± 0.04

Table S9. Glass transition temperatures for PVC plasticized with the diester of 2-ethylhexanol and the listed diacid at a 10 wt. % loading. This table shows the data presented in **Main Text Figure 8** and the control composition with non-bio-derived methyl muconates.

Diacid	Glass Transition Temperature, T_g (°C)	Std. Dev. (°C)
N/A (Neat PVC)	92	± 3
Phthalate Anhydride	32	± 3
Adipic Acid	25	± 3
2-Methyl Muconic Acid	12	± 3
3-Methyl Muconic Acid	9	± 3
2-Methyl Muconic/3-Methyl Muconic (50/50 Molar Blend)	11	± 3
Non-Bio-derived Standard Control Reaction: 2-Methyl Muconic/3-Methyl Muconic (50/50 Molar Blend	9	± 3
2-Methyl Adipic Acid	15	± 3
3-Methyl Adipic Acid	17	± 3
2-Methyl Adipic/3-Methyl Adipic (50/50 Molar Blend)	18	± 3

Table S10. Hazard classifications for EPA T.E.S.T. predictions.

Hazard Indicators	I (highest)	II	III	IV (lowest)
Estrogen receptor (ER) binding	positive			negative
Developmental toxin	positive			negative
Ames Mutagenicity	positive			negative
Oral Rat LD$_{50}$[a]	≤ 50 mg/kg	50 to 500 mg/kg	500 to 5,000	>5,000 mg/kg
Bioconcentration Factor[b]	≥ 5000	1000 to 5000		< 1000
96 hour fathead minnow LC$_{50}$[c]	≤1 mg/L	1 to ≤10 mg/L	>10 to 100 mg/L	> 100 mg/L
48 hour *D. magna* LC$_{50}$[c]	≤1 mg/L	1 to ≤10 mg/L	>10 to 100 mg/L	> 100 mg/L
48 hour *T. pyriformis* IGC$_{50}$[c]	≤1 mg/L	1 to ≤10 mg/L	>10 to 100 mg/L	> 100 mg/L

[a]*Protection of Environment*; Code of Federal Regulations, Title 40, Chapter I, Subchapter E, Part 156, Subpart D, § 156.62

[b]United Nations, *Globally harmonized system of classification and labelling of chemical (GHS), sixth revised edition*; ST/SG/AC.10/30/Rev.6; 2015.

[c]United States Environmental Protection Agency, *Persistent Bioaccumulative Toxic (PBT) Chemicals; Lowering of Reporting Thresholds for Certain PBT Chemicals; Addition of Certain PBT Chemicals; Community Right-to-Know Toxic Chemical Reporting*; 40 CFR Part 372; 1999.

Table S11. Summary of EPA T.E.S.T. predictions. Colors correspond to the hazard levels shown in Table S8. *Abbreviations:* adipic acid, AA; muconic acid, MA; diethylhexyl phthalate DEHP; diethylhexyl adipate, DEHA; diethylhexyl 2-methyl adipate; diethylhexyl 3-methyl adipate, DEH3MA; diethylhexyl muconate, DEHM; diethylhexyl 2-methyl muconate, DEH2MM; diethylhexyl 3-methyl muconate, DEH3MM.

	Tests for human health impacts				Tests for environmental impact			
	ER Binding	Develop. Toxicity	Ames Mutagen	Rat LD$_{50}$ mg/kg	Bioconcent. Factor	Minnow LC$_{50}$ mg/L	*Daphnia* LC$_{50}$ mg/L	*T. pyriformis* IGC$_{50}$ mg/L
Feed								
o-Cresol				136	11.5	33.4	8.99	121
m-Cresol				265	11.2	35.8	9.42	101
p-Cresol				518	9.3	29.1	6.52	106
Diacids and Oxoalcohols								
2-ethylhexanol				1,720	19.5	31.20	31.20	31.20
phthalic acid				5,130	0.5	29.50	29.50	29.50
adipic acid				4,210	0.2	150.00	168.00	767.00
2-methyl adipic acid				5,950	0.2	103.00	116.00	715.00
3-methyl adipic acid				4,620	0.2	133.00	140.00	715.00
muconic acid				6,200	0.4	47.10	113.00	579.00
2-methyl muconic acid				5,800	0.3	26.50	26.50	26.50
3-methyl muconic acid				5,050	0.3	33.40	33.40	33.40
Plasticizers								
BPA				4,150	117.5	3.22	1.58	5.35
DEHP				31,000	17.8	0.24	1.55	0.09
DEHA				9,750	53.7	0.48	1.09	0.48
DEH2MA				10,100	61.7	0.44	0.79	0.32
DEH3MA				9,890	63.2	0.50	0.88	0.31
DEHM				12,700	19.5	0.03	1.68	0.18
DEH2MM				13,500	9.12	0.02	1.52	0.08
DEH3MM				13,500	9.12	0.02	1.66	0.08

Output from the Environmental Protection Agency (EPA) toxicity estimation software tool (T.E.S.T.) providing predicted results for experimental tests. The tests estrogen receptor (ER) binding, developmental toxicity, and Ames mutagenicity have either positive or negative outcomes, reported by the tool as true or false, and negative/false is the desired outcome corresponding to the lowest hazard category. The bioconcentration factor is defined as the ratio of the chemical concentration in fish to that in water at steady state, and thus lower values correspond to lower hazard. Higher values correspond to lower hazard for the remaining categories: oral rat 50 percent lethal dose (LD$_{50}$), fathead minnow 50 percent lethal concentration (LC$_{50}$) after 96 hours of exposure, *D. magna* LC$_{50}$ after 48 hours, and 50 percent growth inhibition concentration (IGC$_{50}$) after 48 hours for *T. pyriformis*.

References

1.   L. N. Jayakody, C. W. Johnson, J. M. Whitham, R. J. Giannone, B. A. Black, N. S. Cleveland, D. M. Klingeman, W. E. Michener, J. L. Olstad, D. R. Vardon, R. C. Brown, S. D. Brown, R. L. Hettich, A. M. Guss and G. T. Beckham, *Energy Environ. Sci.*, 2018, **11**, 1625-1638.
2.   C. W. Johnson and G. T. Beckham, *Metab. Eng.*, 2015, **28**, 240-247.
3.   H. M. Salis, E. A. Mirsky and C. A. Voigt, *Nat. Biotechnol.*, 2009, **27**, 946-950.
4.   P. Puigbo, E. Guzman, A. Romeu and S. Garcia-Vallve, *Nucleic Acids Res.*, 2007, **35**, W126-131.
5.   K.-H. Choi, A. Kumar and H. P. Schweizer, *J. Microbiol. Methods*, 2006, **64**, 391-397.
6.   A. J. Pandell, *J. Org. Chem.*, 1976, **41**, 3992-3996.
7.   A. B. McKague, *Synth. Commun.*, 1999, **29**, 1463-1475.
8.   J. M. Carraher, T. Pfennig, R. G. Rao, B. H. Shanks and J.-P. Tessonnier, *Green Chem.*, 2017, **19**, 3042-3050.
9.   D. R. Vardon, N. A. Rorrer, D. Salvachúa, A. E. Settle, C. W. Johnson, M. J. Menart, N. S. Cleveland, P. N. Ciesielski, K. X. Steirer, J. R. Dorgan and G. T. Beckham, *Green Chem.*, 2016, **18**, 3397-3413.
10.   T. M. Martin, *U.S. Environmental Protection Agency*, 2020.
11.   U. S. EPA, *Chemical Transformation Simulator (CTS), Version 1.0*, 2019.
12.   J. E. Prior, M. D. Lynch and R. T. Gill, *Biotechnol. Bioeng.*, 2010, **106**, 326-332.
13.   C. W. Johnson, D. Salvachúa, N. A. Rorrer, B. A. Black, D. R. Vardon, P. C. St. John, N. S. Cleveland, G. Dominick, J. R. Elmore, N. Grundl, P. Khanna, C. R. Martinez, W. E. Michener, D. J. Peterson, K. J. Ramirez, P. Singh, T. A. VanderWall, A. N. Wilson, X. Yi, M. J. Biddy, Y. J. Bomble, A. M. Guss and G. T. Beckham, *Joule*, 2019, **3**, 1523-1537.